Ferrite LTCC-Based Antennas for Tunable SoP Applications

Atif Shamim, *Member, IEEE*, Joey R. Bray, *Member, IEEE*, Nasrin Hojjat, and Langis Roy, *Member, IEEE*

Abstract—For the first time, ferrite low temperature co-fired ceramic (LTCC) tunable antennas are presented. These antennas are frequency tuned by a variable magnetostatic field produced in a winding that is completely embedded inside the ferrite LTCC substrate. Embedded windings have reduced the typically required magnetic bias field for antenna tuning by over 95%. The fact that large electromagnets are not required for tuning makes ferrite LTCC with embedded bias windings an ideal platform for advanced tunable system-on-package applications. Measurements of rectangular microstrip patch antennas on a ferrite LTCC substrate display a maximum tuning range of 610 MHz near 12 GHz. Two different bias windings and their effect on the antenna performance are discussed, as is the effect of antenna orientation with respect to the bias winding. The antenna radiation patterns are measured under biased and unbiased conditions, showing a stable co-polarized linear gain.

Index Terms—Embedded transformer, ferrite low temperature co-fired ceramic, magnetic properties, tunable antenna.

I. INTRODUCTION

WITH the ever growing need for compact, highly integrated and small size transceiver systems in the wireless industry, low temperature co-fired ceramic (LTCC) technology offers many attractive features and possibilities to achieve these goals. The size of an LTCC substrate can be reduced considerably because of its 3-D capabilities and because passive components, such as capacitors, resistors, inductors and antennas, can be embedded within it. This makes LTCC an ideal medium for system-on-package (SoP) applications [1]. Efficient passive elements can be designed in LTCC because of its low losses. The introduction of a high-dielectric constant ferrite material in the package not only helps to miniaturize the components but also permits the control of the devices made from it. Ferrite allows the properties of the package to be dynamically altered, meaning

A. Shamim is with the Department of Electrical Engineering, King Abdullah University of Science and Technology, Thuwal 23955, Saudi Arabia (e-mail: atif.shamim@kaust.edu.sa).

J. R. Bray is with the Department of Electrical and Computer Engineering, Royal Military College of Canada, Kingston, ON K7K 7B4, Canada (e-mail: joey.bray@rmc.ca).

N. Hojjat is with the TenXc Wireless Inc., Ottawa, ON K2K 2X1, Canada (e-mail: nhojjat@tenxc.com).

L. Roy is with the Department of Electronics, Carleton University, Ottawa, ON K1S 5B6, Canada (e-mail: lroy@doe.carleton.ca).

that the package will have the ability to control the signals that are passing through it [2], [3]. Therefore, ferrite LTCC is a perfect candidate for tunable passive elements. This SoP work is an attempt to push the package beyond merely providing embedded passives, wiring and physical protection, the package itself becomes the device. This concept is useful for applications such as direct broadcast satellite television (DBS-TV) reflectarrays, where reconfigurable coverage is required or for multi-band wireless sensor systems.

Ferrite integration in an LTCC medium is a recent concept. A limited number of experimental ferrite tape materials are currently available and can be used as stand-alone systems or sandwiched between standard LTCC dielectric layers. Our previous work [4] focused on the extraction of material properties for an experimental ferrite LTCC tape system, ESL 40012 [5]. This paper furthers the work by investigating the suitability of ferrite LTCC for tunable antennas and SoP designs.

Although antennas printed on ferrite substrates have been previously documented, most have relied on traditional ferrite substrates that are inherently difficult to magnetize. Unbiased ferrite substrates and self-magnetized thin films have been investigated as a means of reducing the size of antennas owing to the high permittivity of the ferrite medium [6]–[8]. Frequency tuning of antennas has been demonstrated by biasing the ferrite substrate [9]–[15]. Pattern and polarization control of ferrite-based antennas have also been successfully achieved [16]–[18]. In [19], patch antennas on non-uniformly biased ferromagnetic substrates have been analyzed. Recently, a switchable ferrite microstrip antenna array has been presented [20]. However, most of the documented antennas operate in the magnetically saturated state. Given that the antennas are fabricated on traditional ferrite substrates, large external permanent magnets or electromagnets must be used to provide the high magnetostatic fields, the latter being commensurate with the demagnetization factors of the substrate. Typical external magnetic field intensities H are in the order of 80 kA/m (1000 Oe) and the large size of the required magnets makes the system extremely bulky and unsuitable for compact SoP applications. Unlike the previous work, the tunable antennas presented in this paper are fabricated on a multilayer ferrite LTCC substrate with bias windings that are completely embedded within the same substrate. Demagnetization factors are largely absent from such an arrangement, which greatly lowers the magnetostatic field strength required for tuning. Additionally, the antennas operate at a sufficiently high frequency such that low-field losses are negligible, implying that unsaturated ferrite regions

Fig. 1. Two patch antennas on a ferrite substrate, where the magnetic field inside the substrate H_0 is represented by dashed lines: (a) longitudinal and (b) transverse patch orientations.

TABLE I
MEASURED RELATIVE PERMITTIVITY ε_r AND LOSS TANGENT tan δ

	Frequency (GHz)	Thickness ($t \pm \mathrm{d}t$) μm	$\varepsilon_r \pm d\ \varepsilon_r$	tan $\delta \pm$ d tan δ 10^{-3}
Sample 1	9.86	230 ± 10	13.70 ± 0.59	4.24 ± 0.37
Sample 2	27.2	230 ± 10	14.14 ± 0.65	1.11 ± 0.10

within the LTCC substrate are tolerable, which further serves to reduce the required magnetostatic field strength. This novel approach enables tuning of the antennas with modest field strengths in the order of only 2 kA/m (25 Oe), which is a reduction of more than 95%.

Section II introduces the theory of ferrite antennas and presents the tunable antenna design along with the biasing structures. Impedance measurements are presented in Section III, whereas Section IV presents the gain and radiation pattern measurements. Various design parameters and tradeoffs are investigated. The challenges associated with the radiation pattern and gain measurements of these antennas under biased conditions are also reported. Section V briefly presents future work efforts on ferrite integration for SoP applications.

II. THEORY AND DESIGN

A. Theory

Ferrite-based antennas typically use a variable magnetostatic bias to achieve tunability and re-configurability [21], [22]. For such antennas, the resonance frequency variation is dependent on the bias direction and strength [23]. Usually, ferrite materials at microwave frequencies are used in the saturated state. In this regime, the well-known Polder equations [24] are used to represent the permeability tensor of the ferrite in terms of the applied internal magnetostatic field (H_0) and the saturation magnetization (M_s). These equations indicate that the elements of the permeability tensor exhibit a resonance around a specific frequency, called the Larmor frequency f_0, which is proportional to H_0. Ferrite is very lossy in the vicinity of its Larmor frequency, thus it is customary to operate the ferrite above this frequency for microwave applications, even though the ability to tune the ferrite decreases with frequency in this range [25]. Previous characterization efforts have revealed that an internal H_0-field of over 2500 A/m is required to fully saturate ESL 40012 ferrite LTCC to its magnetization value of $\mu_0 M_s = 400$ mT. Providing such a high, uniform bias field within a miniature LTCC package is quite challenging without the use of a bulky external magnet. Failure to fully saturate the ferrite results in additional low-field losses, which are incurred approximately up to the magnetization frequency $f_m = (2.8 \times 10^{10}$ Hz/T$) \cdot \mu_0 M_s = 11.2$ GHz

for this particular ferrite material. Given the unlikelihood of achieving a uniformly high bias level, an operating frequency of 12 GHz was chosen such that low-field losses will be avoided altogether [4].

Due to their anisotropic behavior, ferrites display different properties depending on the orientation of H_0 with respect to the direction of both the wave propagation and the radio frequency (RF) magnetic field [9], [14]. Two different patch antenna orientations are investigated with respect to H_0, as shown in Fig. 1. In the first case, the antenna and its microstrip feed line are placed in a longitudinal orientation with respect to H_0, whereas in the second case the antenna is transverse to the H_0 field.

In most of the previous investigations, the ferrites are biased to saturation with the use of high external bias fields in the order of 80 kA/m, which is usually accomplished by the external electromagnets or permanent magnets [9], [11], [13]. This is not a suitable method for SoP applications. In the proposed design, the ferrite underneath the patch antennas will be partially biased using embedded electromagnet windings. By producing the magnetostatic field within the ferrite itself, the demagnetization factors that act to reduce the internal H_0 field are absent. Magnetostatic measurements have revealed that a relatively low DC current of no more than 500 mA is sufficient to generate magnetic field strengths in the order of 2 kA/m (25 Oe) within the core of the windings [4]. Tunability of the antenna will be achieved by varying the current flowing through the windings. This methodology has been used successfully in our previous ferrite LTCC work [4].

B. Ferrite LTCC Material Properties

Two samples of unbiased ferrite LTCC have been tested and characterized to obtain their microwave properties [4]. Due to the sample size constraints, the lowest measurement frequency was 9.86 GHz. Table I presents the relative permittivity ε_r and loss tangent tan δ parameters for the two samples at two frequencies, 9.86 and 27.2 GHz. In both cases, the relative permeability μ_r is found to be 1 and the average relative permittivity is 13.9. The loss tangents are in the order of 10^{-3}, indicating that this ferrite may be used to build low-loss microwave circuits.

In addition to the resonant cavity method, the thru-reflect-line calibration technique has also been used with printed coplanar waveguide (CPW) lines to assess the transmission line losses using the ferrite under test. The attenuation constant α was extracted from the calibration structures built on the ferrite substrate. Except for the 2–9 GHz band, α values of
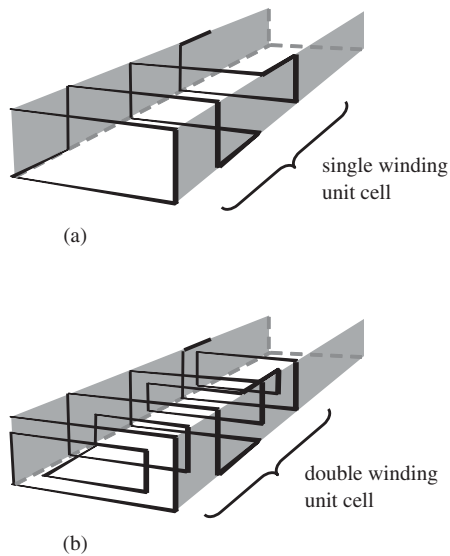
Fig. 2. Conceptual LTCC biasing transformer windings: (a) single loop unit cell used for the secondary winding and (b) double loop unit cell used for the primary winding.

Fig. 3. (a) Cross section of the 10-layer LTCC stack showing the double-loop primary winding and the single-loop inner secondary winding. (b) Top view of the solenoid windings. (c) Top view of the toroid windings.

approximately 0.5 dB/cm are obtained which confirm the low loss behavior of this material. Losses peaked at approximately 7 GHz and are due to the resonance of domain wall rotation inside the ferrite, a phenomenon that is related to low-field losses in unsaturated polycrystalline ferrites. For practical circuit applications in the 2–9 GHz band, the domain wall resonance and associated loss must be removed by saturating the ferrite material [9]. This problem is avoided altogether if the intended application requires an operating frequency that is greater than f_m.

C. Biasing Transformers

In order to bias the ferrite LTCC antennas, only one of the transformer windings (the primary) is required. However, a complete transformer has been designed inside the substrate in order to characterize the internal $B(H)$ hysteresis response of the ferrite. Two different types of transformers have been used, the first being a straight solenoid transformer completely embedded within the ferrite LTCC material, similar to previous work [2]. The secondary winding uses a single loop, whereas the primary winding uses a double loop, as shown in Fig. 2(a) and (b), respectively. The front cross-sectional view of a unit cell is shown in Fig. 3(a). The turns are made of 200-μm wide silver conductors that are connected using 150-μm diameter vias, and the pitch between the conductors is 375 μm. The complete transformer fits into a 10-layer ferrite LTCC module with each layer being 124 μm thick. In order to fit the solenoid transformer in a maximum permissible part size of 20 mm × 20 mm, 11 unit cells are used. The solenoid uses 77 primary and 33 secondary turns which requires a total of 1198 transitions and 1108 vias.

A finite-length solenoid is subjected to end-effects that can introduce errors in the measurements. Further, leakage out of the sides of the solenoid is also a concern, which can potentially lead to overestimates of the flux inside its core.
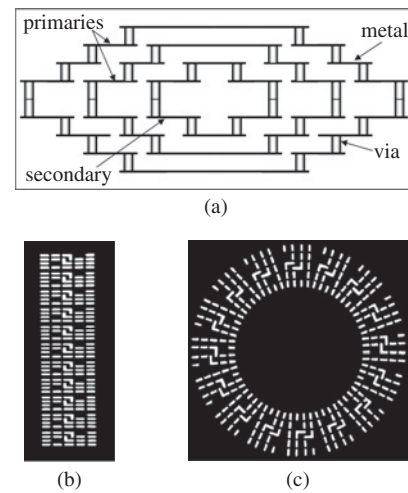
A toroid, on the other hand, entirely encloses the magnetic fields within its core and is less prone to leakage effects. A toroid transformer has also been designed in which unit cells are closely spaced and the fields are more tightly contained within the windings. A total of 112 primary turns and 48 secondary turns are completely embedded in 10-ferrite LTCC layers. The inner diameter of the toroid transformer is 10.3 mm and the outer diameter is 18.7 mm. It has 16 unit cells, which are spaced at 171 μm on the inner radius and 1.28 mm at the outer radius. The top view of one of the layers (from the layout file) of the solenoid and of the toroid is shown in Fig. 3(b) and (c), respectively.

The hysteresis measurement procedure consists of incrementing the primary current periodically and recording the corresponding secondary voltages which are then converted to actual values of H and magnetic flux density B, respectively [4]. The results are then plotted to obtain the $B(H)$ curves for every current setting. Antenna tuning occurs at a much lower frequency than the RF frequency that is radiated by the antenna, hence the $B(H)$ curves should be measured at a frequency that is close to DC. In this experiment, a frequency of 1 kHz was sufficient to provide measurable voltages on the secondary winding.

The major $B(H)$ curve of the solenoid, measured at saturation, shown in Fig. 4 by the dashed line was obtained by energizing the primary winding with a peak current of 650 mA. Based on the solenoid measurements, the saturation flux density B_s is 330 mT for an applied magnetic field of 2.1 kA/m. The remanent flux density B_r is 180 mT, the squareness is 0.55, and the coercive magnetic field H_c is 520 A/m. The same procedure has been used for the toroid. Due to the curvature of the toroid, the turn density of its primary winding is lower than that of the solenoid by a factor of 0.6. The major hysteresis curve for the toroid is shown by the solid line in Fig. 4.

A comparison of the curves in Fig. 4 indicates that ESL 40012 is easier to magnetize with the toroid than it is with the solenoid. This is expected since the toroid suffers from less
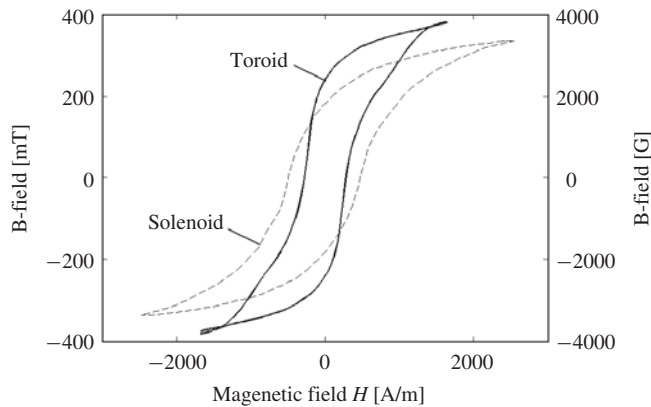
Fig. 4.   Measured hysteresis curves from the LTCC transformers.
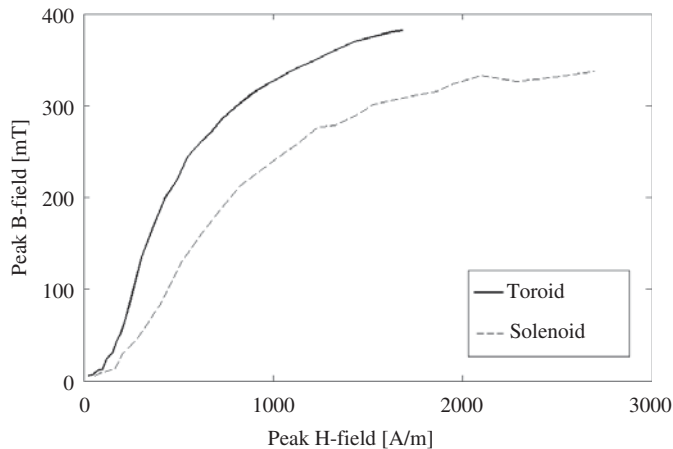
Fig. 5.   Measured peak B-field versus peak H-field for ESL 40012 LTCC.

leakage effects than the solenoid. This difference is clearly evident in Fig. 5, which plots the peak B-field versus the peak H-field for each current setting. Although saturation could not quite be achieved with the toroid, the trend clearly indicates that the saturation flux density B_s approaches 400 mT instead of the 330 mT obtained using the solenoid. For the toroid, $B_r = 250$ mT, the squareness is approximately 0.63, and $H_c \approx 330$ A/m.

D. Antenna Design

Microstrip patch antennas designed to operate at 12 GHz have been fabricated on the same substrates that were used to obtain the hysteresis curves. Note that the embedded windings between the patch and the ground plane will likely perturb the patch antenna's microwave response. However, simulating the windings (more than 1100 vias) and the non-uniform fields that they create is an intractable problem. Given this, recourse to experimental measurements was used to provide the proof of concept for this paper. The cross-sectional view of the ferrite LTCC tunable antenna is shown in Fig. 6. The module consists of 10 layers of ferrite LTCC ($h_1 = 1.09$ mm) out of which the bias windings occupy eight layers ($h_2 = 0.87$ mm). The microstrip-fed rectangular patch antennas were made of copper on the top layer of the substrate by a post-processing milling step. The bottom of the substrate contains the ground plane.
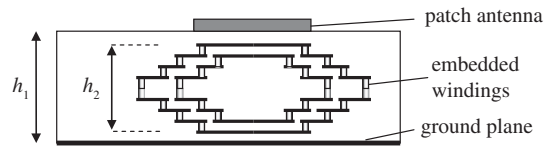
Fig. 6.   Cross sectional view of the tunable antenna module.
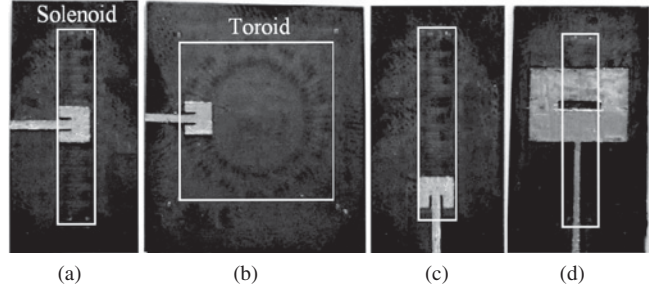
Fig. 7.   Fabricated antennas on ESL 40012 ferrite LTCC, where the white boxes show the locations of the embedded windings. (a) Transverse small patch on solenoid. (b) Transverse small patch on toroid. (c) Longitudinal small patch on solenoid. (d) Longitudinal large slotted patch on solenoid.

Different antenna designs and orientations have been investigated, as shown in Fig. 7. Microstrip-fed patch antennas operating at their first resonance have been placed transversally over both the solenoid [Fig. 7(a)] and toroid [Fig. 7(b)] windings. An identical patch has also been placed longitudinally over the solenoid [Fig. 7(c)]. In order to investigate the performance of a larger-sized antenna that can completely cover the solenoid winding beneath it, a second patch design operating in its 3rd resonance at 12 GHz is shown in Fig. 7(d), where the slot in the center of the patch is used to increase its electrical length such that the patch fits it in the available substrate space.

III. IMPEDANCE MEASUREMENTS

An Anritsu 3680-20 universal test fixture is used to make the transition from the network analyzer's coaxial cable to the microstrip line that feeds the patch antenna, as shown in Fig. 8. The winding within the LTCC substrate is biased with DC current supplied through probes that contact two pads on the top layer of the substrate that lead to the windings. The reflection scattering parameter (S_{11}) of each antenna is measured using the network analyzer as a function of the applied bias current, which is increased in 50 mA increments until the maximum current level is reached, being 500 mA for the antennas over the solenoid [Fig. 7(a), (c), and (d)] and 700 mA for the antenna over the toroid [Fig. 7(b)].

The tuning response of one of the antennas, the small patch oriented transversely over the embedded solenoid [Fig. 7(a)], is shown in Fig. 9, where Fig. 9(a) shows the wideband response of the antenna at only the minimum (0 mA) and maximum (500 mA) bias settings. Multiple resonances are apparent in each of the two curves in Fig. 9(a). The desired patch mode is identified by examining the 0 mA curve and finding the measured resonant frequency that most closely matches the predicted resonant frequency of the antenna. In Fig. 9(a), the resonance at 11.99 GHz is the closest to the predicted
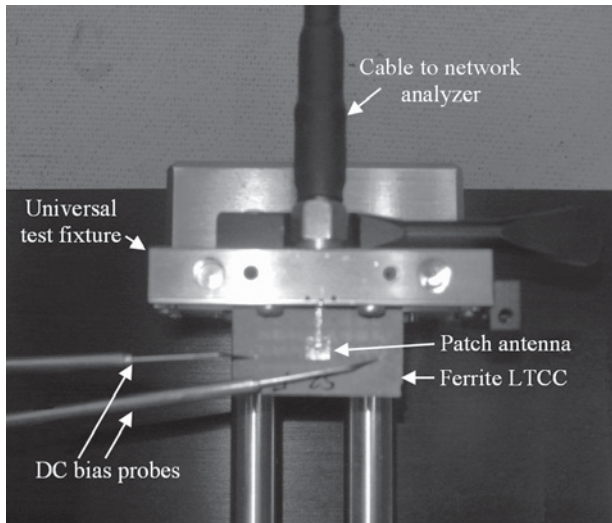
Fig. 8. Ferrite LTCC substrate and patch antenna mounted on the universal test fixture, with the bias probes contacting the substrate's DC pads.

(a)

(b)
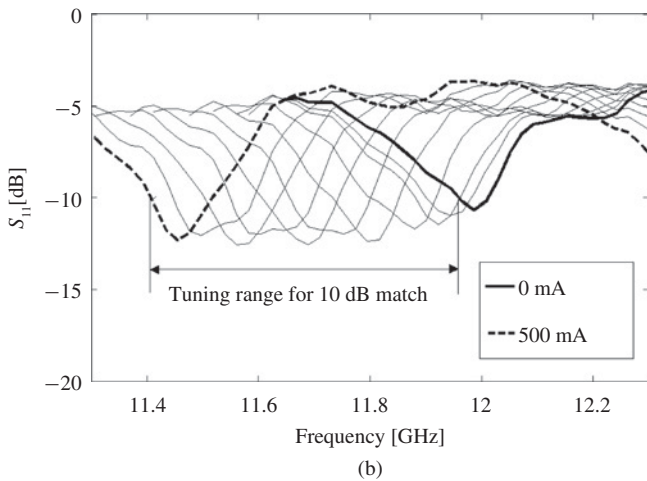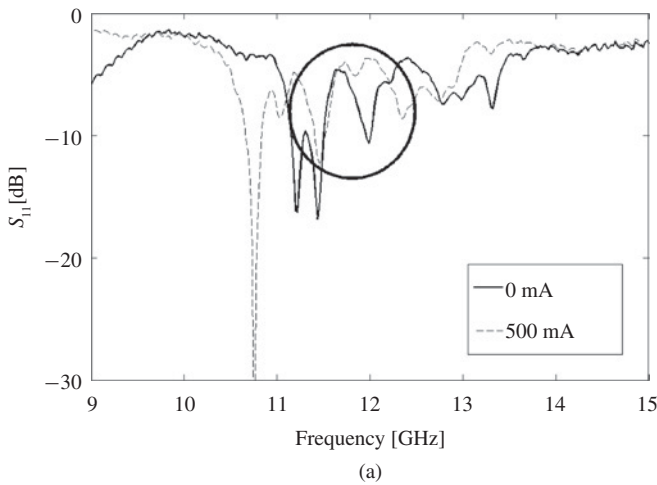
Fig. 9. Measured input match of the antenna in Fig. 7(a). (a) 9–15 GHz range and (b) within the encircled patch resonance, where the unlabeled intermediate lines represent 50-mA increments of the bias current.

frequency of 12.0 GHz. The other resonant dips in Fig. 9(a) are associated with surface modes, volume resonances or higher-order patch modes that do not radiate efficiently [9], [11].

TABLE II
SUMMARY OF ANTENNA IMPEDANCE TUNING

Antenna Shown in	Resonant Frequency, Zero Bias (GHz)	Resonant Frequency at Max. Bias (GHz)	Tuning Bandwidth (MHz)
Fig. 7(a)	11.99	11.46	530 (4.4%)
Fig. 7(b)	12.18	11.60	580 (4.8%)
Fig. 7(c)	12.39	12.07	320 (2.6%)
Fig. 7(d)	12.11	11.50	610 (5.0%)

TABLE III
COMPARISON OF TUNING USING A FERRITE PATCH ANTENNA

Reference	Magnetic Field Strength	Tuning (GHz)	Tuning Bandwidth with Respect to Zero Bias
[9]	Unknown	2.8−4.6	39%
[11]	600 kA/m	0.2−1.0	400%
[15]	1.6 kA/m	2.12−2.13	0.5%
This work	2 kA/m	11.5−12.1	5%

The patch mode resonance at 11.99 GHz was further confirmed by moving a reflector above the patch and noting that only this resonance displayed a significant response to the moving reflector. The highlighted area within the circle in Fig. 9(a) has been expanded in Fig. 9(b), which shows the responses produced by all of the bias level settings in 50 mA increments.

The measured tuning ranges of the four antennas shown in Fig. 7 are listed in Table II. The resonant frequencies of the measured antennas decrease as a function of the applied bias current, regardless of the direction of the magnetic bias field (transverse or longitudinal compared to the microstrip feed line) and regardless of the direction of the DC current (positive or negative). Of the small patch antennas, the ones that had their H_0 bias field oriented transversely to the antenna feed line [Fig. 7(a) and (b)] had the highest tuning range (530–580 MHz), whereas the small antenna with the bias field oriented longitudinally to the feed line [Fig. 7(c)] had the lowest tuning range of 320 MHz. The observation that the transverse bias provides more tuning than the longitudinal bias is in agreement with that in [9]. The large patch antenna with the slot [Fig. 7(d)] has a tuning range of 610 MHz despite its use of a longitudinal bias. It is believed that if this antenna is placed in the transverse orientation with respect to H_0, it will provide a tuning range in excess of 610 MHz.

The measured 530–610 MHz tuning ranges presented in Table II are approximately 5% of the unbiased resonant frequencies. The tuning ranges of similar rectangular ferrite patch antennas are listed in Table III. Although higher tuning ranges have been demonstrated, these have only been accomplished using permanent magnets [9] or very large electro-magnets [11]. The 5% tuning range demonstrated here has been accomplished using a modest magnetic field of 2 kA/m.
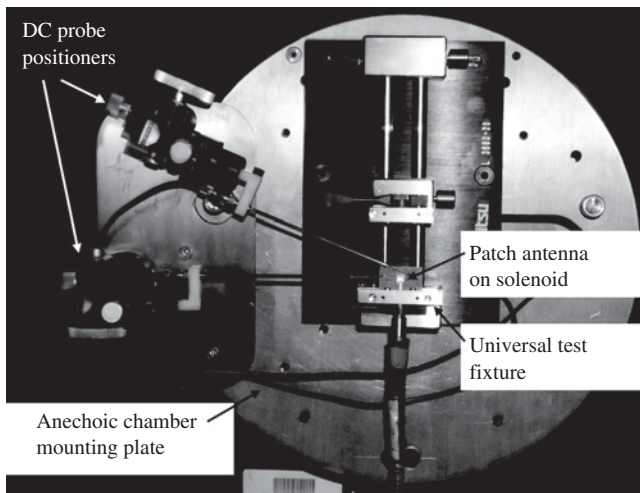
Fig. 10. Ferrite patch antenna, universal test fixture and DC probes installed on the anechoic chamber mounting plate for radiation pattern measurements (absorber removed for clarity).

Furthermore, this paper is the only reported one that uses a winding that is part of the antenna structure itself.

The results are encouraging given that the windings in the ferrite have not been optimized for tuning—they are merely the same transformer cores that were used to characterize the ferrite. Note that the antennas do not require continuous current to operate. A current pulse may be used to go from one tuning state to the other, as the material has significant remanence to hold the magnetization (as is clear from the hysteresis curve shown in Fig. 4), albeit for high bias currents. Substantial reductions of bias current are expected if the bias windings and their placement are optimized for antenna applications.

IV. Gain and Radiation Pattern Measurements

A challenging part of characterizing the ferrite-based tunable antennas is measuring their gain and radiation patterns under biased conditions. This is because the antennas have to be mounted and rotated in the anechoic chamber along with the DC probes that are required to bias the windings underneath the antenna. A custom mount has been made for this purpose as shown in Fig. 10. The DC probes are mounted on a metallic plate and this plate is then screwed to the large rotating base plate in the anechoic chamber. The universal test fixture has also been attached to the base plate. The antennas are fed through the universal test fixture and biased through the probes. A horn antenna acts as the transmit antenna at the other side of the chamber. At certain angles the probes blocked the radiation pattern measurement, however, the testing is not affected by the presence of the probes in most of the measurement scans. This fact is established by doing two sets of measurements, one with and the other without the probes. The measurements are preceded by the calibration procedure which is done using two horn antennas in the 12–13 GHz frequency range.

The measured normalized radiation patterns in the E-plane and H-plane for the transverse patch on the solenoid [Fig. 7(a)]
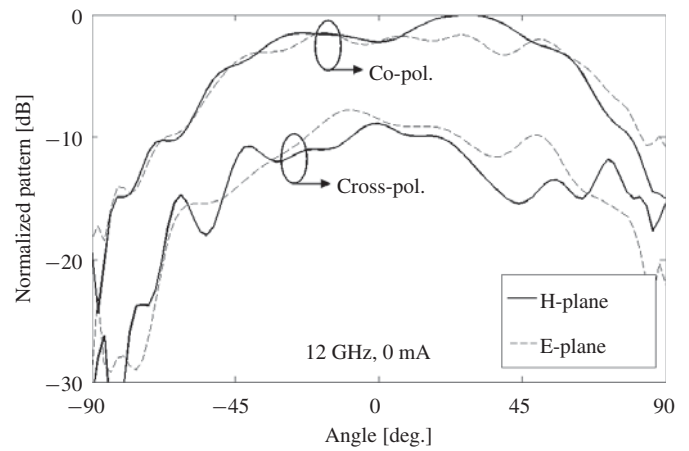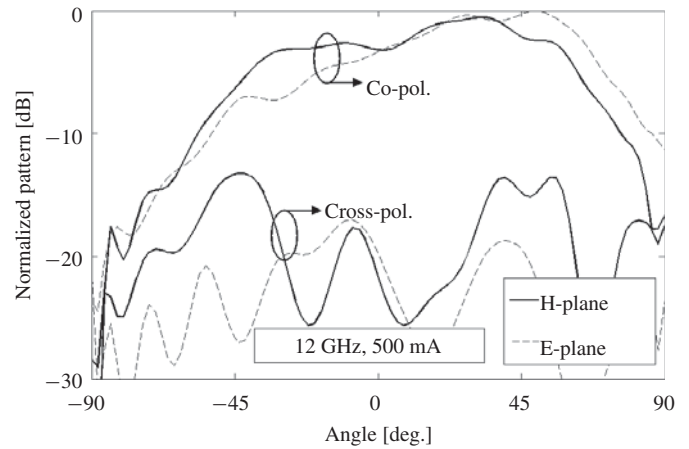
Fig. 11. Ferrite antenna measured normalized (co-pol and cross pol) radiation pattern of the small transverse patch antenna over the solenoid [Fig. 7(a)] in the H- and E-planes at 12.0 GHz for (a) no bias and (b) +500 mA bias.

are shown in Fig. 11(a) in the unbiased state at 12.0 GHz. Similar patterns were recorded at other frequencies. The maximum gain is approximately -0.6 dBi, which is lower than expected because of the likely existence of surface waves on the thick ferrite substrate, as explained in the next paragraph. The cross-polarization levels are less than 8 dB below the co-polarized levels at boresight. The high cross-polarization levels, also noted in [9] and [10], are typical of ferrite patches because of the gyrotropic nature of the ferrite.

The ripples in the radiation patterns and lower than expected gain values are likely due to surface wave excitation. The surface waves launched by the patch antenna radiate when they meet the edges of the substrate and this radiation interferes with the main radiation pattern, which is expected to be hemispherical and smooth for a rectangular patch. Surface waves are always present on a grounded substrate due to the zero-frequency cutoff of the TM_0 surface wave mode. Surface wave losses on high dielectric constant substrates can be minimized by limiting the substrate thickness to being much less than 10% of the free-space wavelength, $h << 0.1\lambda_0$, or $h < 0.005\lambda_0$ [26]. However, the substrate used in this paper ($h = 1.09$ mm) is approximately $0.044\lambda_0$ at 12.0 GHz, over

eight times the limiting value, indicating the likely presence of surface waves.

Changing the bias level at a given frequency is shown in Fig. 11(b), where the bias has been increased to +500 mA. Apart from a slight squint in the E-plane toward positive angles, the application of the transverse bias does not significantly alter the co-polarized patterns, which is in agreement with [10]. However, the cross-polarization is significantly affected by the bias, again in agreement with that in [10], where the cross-polarized levels are now less than 14 dB below the co-polarized patterns near boresight. Hence the application of bias is beneficial in controlling the cross-polarization levels.

Measurements of the large patch antenna with the slot [Fig. 7(d)] suffered the most due to blockage from the probes. The radiation pattern of the toroid-based antenna appeared to be the smoothest and resembled the typical patch antenna pattern, however, the gain values were slightly lower.

V. FERRITE LTCC SoP FUTURE WORK

Placing the bias windings below the ground plane instead of between the antenna and the ground plane will be beneficial in two ways. Firstly, the spacing h_1 between the patch and the ground can be reduced, thereby reducing the substrate mode coupling and improving the smoothness of the radiation patterns. Secondly, the high-frequency simulation of the antenna would be greatly simplified, as the effects of the windings greatly complicate the simulation of the structure. Although moving the bias winding may weaken the bias field and thereby reduce the tuning range, the estimation of the magnetostatic bias field under the antenna will be greatly simplified in this configuration, permitting a better theoretical prediction of the antenna's performance. This is left as future work.

The low loss tangent of the ESL ferrite, coupled with the high value of ε_r, implies that this ferrite material, even in its unbiased state, is useful for miniaturizing microwave circuits and antennas. However, the true advantage of ferrite LTCC is its ability to change its permeability tensor with applied magnetic bias, thereby giving an additional dimension of tuning freedom to microwave designers. As previously mentioned, the performance of ferrite LTCC-based antennas can be improved by the co-design of the antenna and its underlying winding. New configurations for the bias windings are currently being explored, along with alternate radiators such as CPW patches, slots and dielectric resonators, all embedded in the LTCC package.

Although not shown here, microstrip line measurements have demonstrated significant phase and amplitude variations with bias. Ferrite LTCC-based patch antennas are therefore ideal candidates for reconfigurable reflectarrays. In addition, the amplitude variations may be used to build other switchable devices. Finally, several other possibilities exist for tunable microwave components inside an LTCC SoP, including tunable lumped element inductors for the realization of tunable filters and matching networks.

VI. CONCLUSION

ESL 40012 experimental ferrite LTCC tape has been used for the first time to realize tunable antennas. These antennas are tuned through completely embedded bias winding that reduced the typically required bias values of 80 kA/m to only 2 kA/m, a reduction of over 95%. The use of an embedded bias winding also negates the requirement of bulky magnets, thus making ferrite LTCC and ideal candidate for compact, tunable SoP. The measured results demonstrate a maximum resonant frequency tuning range of 610 MHz using a non-optimized bias winding and an antenna gain of −0.6 dBi has been measured. Based on experimental results, ferrite LTCC appears to be a promising platform for tunable SoP modules.

REFERENCES

[1] A. Shamim, M. Arsalan, L. Roy, M. Shams, and G. Tarr, "Wireless dosimeter: System-on-chip versus system-in-package for biomedical and space applications," *IEEE Trans. Circuits Syst. II*, vol. 55, no. 7, pp. 643–647, Jul. 2008.

[2] J. R. Bray, K. T. Kautio, and L. Roy, "Characterization of an experimental ferrite LTCC tape system for microwave and millimeter-wave applications," *IEEE Trans. Adv. Packag.*, vol. 27, no. 3, pp. 558–565, Aug. 2004.

[3] J. R. Bray and L. Roy, "Development of a millimeter-wave ferrite-filled antisymmetrically biased rectangular waveguide phase shifter embedded in low-temperature cofired ceramic," *IEEE Trans. Microw. Theory Tech.*, vol. 52, no. 7, pp. 1732–1739, Jul. 2004.

[4] A. Shamim, J. Bray, N. Hojjat, R. A. Elasoued, and D. Baillargeat, "Microwave and magnetostatic characterization of ferrite LTCC for tunable and reconfigurable SiP applications," in *Proc. IEEE MTT-S Int. Microw. Symp.*, Honolulu, HI, Jun. 2007, pp. 691–694.

[5] *ESL Electro-Science Specification Data Sheet: Magnetic Tape 40012* [Online]. Available: http://www.electroscience.com/pdf/40012.pdf

[6] S. Das and S. Chowdhury, "Rectangular microstrip antenna on a ferrite substrate," *IEEE Trans. Antennas Propag.*, vol. 30, no. 3, pp. 499–502, May 1982.

[7] N. Das, S. Chowdhury, and J. Chatterjee, "Circular microstrip antenna on ferrimagnetic substrate," *IEEE Trans. Antennas Propag.*, vol. 31, no. 1, pp. 188–190, Jan. 1983.

[8] G.-M. Yang, X. Xing, A. Daigle, O. Obi, M. Liu, J. Lou, S. Stoute, K. Naishadham, and N. X. Sun, "Planar annular ring antennas with multilayer self-biased NiCo-ferrite films loading," *IEEE Trans. Antennas Propag.*, vol. 58, no. 3, pp. 648–655, Mar. 2010.

[9] D. M. Pozar and V. Sanchez, "Magnetic tuning of a microstrip antenna on a ferrite substrate," *Electron. Lett.*, vol. 24, no. 12, pp. 729–731, Jun. 1988.

[10] P. J. Rainville and F. J. Harackiewicz, "Magnetic tuning of a microstrip patch antenna fabricated on a ferrite film," *Microw. Guided Wave Lett.*, vol. 2, no. 12, pp. 483–485, Dec. 1992.

[11] R. K. Mishra, S. S. Pattnaik, and N. Das, "Tuning of microstrip antenna on ferrite substrate," *IEEE Trans. Antennas Propag.*, vol. 41, no. 2, pp. 230–233, Feb. 1993.

[12] H. How, P. Rainville, F. Harackiewicz, and C. Vittoria, "Radiation frequencies of ferrite patch antennas," *Electron. Lett.*, vol. 28, no. 15, pp. 1405–1406, Jul. 1992.

[13] A. Petosa, R. K. Mongia, M. Cuhaci, and J. S. Wight, "Magnetically tunable ferrite resonator antenna," *Electron. Lett.*, vol. 30, no. 13, pp. 1021–1022, Jun. 1994.

[14] C. F. L. Vasconcelos, S. G. Silva, M. R. M. L. Albuquerque, A. G. d'Assuncao, and J. R. S. Oliveira, "Ferrite substrate in patch antennas for millimeter wave applications," in *Proc. SBMO/IEEE MTT-S Int. Microw. Optoelectron. Conf.*, Belem, Brazil, Nov. 2009, pp. 78–82.

[15] G.-M. Yang, X. Xing, A. Daigle, M. Liu, O. Obi, J. W. Wang, K. Naishadham, and N. X. Sun, "Electronically tunable miniaturized antennas on magnetoelectric substrates with enhanced performance," *IEEE Trans. Magn.*, vol. 44, no. 11, pp. 3091–3094, Nov. 2008.

[16] A. Henderson and J. R. James, "Magnetised microstrip antenna with pattern control," *Electron. Lett.*, vol. 24, no. 1, pp. 45–47, Jan. 1988.

[17] D. M. Pozar, "Radiation and scattering characteristics of microstrip antennas on normally biased ferrite substrates," *IEEE Trans. Antennas Propag.*, vol. 40, no. 9, pp. 1084–1092, Sep. 1992.

[18] T. Fukusako, A. Imahase, and N. Mita, "Polarization characteristics of patch antenna using in-plane and weakly biased ferrite substrate," *IEEE Trans. Antennas Propag.*, vol. 52, no. 1, pp. 325–327, Jan. 2004.

[19] A. D. Brown, J. L. Volakis, L. C. Kempel, and Y. Botros, "Patch antennas on ferromagnetic substrates," *IEEE Trans. Antennas Propag.*, vol. 47, no. 1, pp. 26–32, Jan. 1999.

[20] R. Pourush, G. S. Tyagi, G. P. Srivastava, and P. K. S. Pourush, "Radiation performance of switchable ferrite microstrip array antenna," *IEEE Antennas Wireless Propag. Lett.*, vol. 5, no. 1, pp. 195–198, Dec. 2006.

[21] K. K. Tsang and R. J. Langley, "Design of circular patch antennas on ferrite substrates," *IEE Proc. - Microw. Antennas Propag.*, vol. 145, no. 1, pp. 49–55, Feb. 1998.

[22] N. P. Mahalik, "Tuning procedure in microstrip antennas on ferrite substrate," in *Proc. 10th Int. Conf. Antennas Propag.*, vol. 1. Edinburgh, U.K., Apr. 1997, pp. 294–297.

[23] G. Leon, R. R. Boix, and F. Medina, "Full-wave analysis of a wide class of microstrip resonators fabricated on magnetized ferrites with arbitrarily oriented bias magnetic field," *IEEE Trans. Microw. Theory Tech.*, vol. 50, no. 6, pp. 1510–1519, Jun. 2002.

[24] R. F. Soohoo, *Theory and Application of Ferrites*. Englewood Cliffs, NJ: Prentice-Hall, 1960, pp. 83–111.

[25] W. E. Hord, "Microwave and millimeter-wave ferrite phase shifters," *Microw. J.*, vol. 32, pp. 81–94, Sep. 1989.

[26] N. G. Alexopoulos, P. B. Katehi, and D. B. Rutledge, "Substrate optimization for integrated circuit antennas," *IEEE Trans. Microw. Theory Tech.*, vol. 31, no. 7, pp. 550–557, Jul. 1983.

Atif Shamim (S'03–M'09) received the M.A.Sc. and Ph.D. degrees in electrical engineering at Carleton University, Ottawa, ON, Canada, in 2004 and 2009, respectively.

He was the Natural Sciences and Engineering Research Council of Canada (NSERC) Alexander Graham Bell Graduate Scholar at Carleton University from 2007 to 2009 and an NSERC Post-Doctoral Fellow at King Abdullah University of Science and Technology (KAUST), Thuwal, Saudi Arabia, from 2009 to 2010. He joined the Electrical Engineering Program at KAUST in August 2010, where he is currently an Assistant Professor. He was an Invited Researcher at Valtion Teknillinen Tutkimuskeskus Electronics Micro-Modules Research Center, Oulu, Finland, in 2006. His current research interests include integrated on-chip antennas, low power complementary metal-oxide semiconductor radio frequency integrated circuit for system-on-chip applications and advanced system-on-package designs employing multilayer low temperature co-fired ceramic and liquid crystal polymer packaging technologies.

Dr. Shamim was the recipient of the Best Paper Prize at the European Wireless Technology Conference in the European Microwave Association Week in 2008. He was given the Ottawa Centre of Research Innovation Researcher of the Year Award in 2008. His work on "Wireless Dosimeter" won the Information Technology Association of Canada Strategic Microelectronics Council Award at the Canadian Microelectronics Corporation TEXPO in 2007. He received the Best Student Paper Finalist Prize at the IEEE Antennas and Propagation Society Conference in 2005.

Joey R. Bray (S'96–M'04) received the B.A.Sc. and M.A.Sc. degrees in electrical engineering from the University of Ottawa, Ottawa, ON, Canada, in 1995 and 1998, respectively, and the Ph.D. degree in electrical engineering from Carleton University, Ottawa, in 2003.

He joined the Department of Electrical and Computer Engineering, Royal Military College of Canada, Kingston, ON, Canada, in 2003, where he is currently an Associate Professor. He was a Visiting Researcher at Valtion Teknillinen Tutkimuskeskus Electronics, Oulu, Finland, from 2001 to 2002. During his sabbatical leave from 2010 to 2011, he was a Visiting Research Associate at the School of Electrical and Electronic Engineering, University of Manchester, Manchester, U.K. His current research interests include nonreciprocal microwave devices, ferrites and ceramic packaging.

Dr. Bray received the Young Scientist Award in 2005 from the International Union of Radio Science.

Nasrin Hojjat received the B.Sc., M.Sc., and Ph.D. degrees in electromagnetic/microwave engineering from the University of Tehran, Tehran, Iran, in 1989, 1991, and 1997, respectively. She was preparing her Ph.D. thesis at the University of Waterloo, Waterloo, ON, Canada, from 1993 to 1994.

She was performing research on mm-wave antennas as a Post-Doctoral Fellow at the University of Waterloo from 1998 to 1999. She was employed as a Lecturer at the University of Tehran from 1992 to 1998, and as an Assistant Professor from 2000 to 2004. From 2004 to 2006, she was performing research on low temperature co-fired ceramic (LTCC), reconfigurable antennas and electromagnetic compatability/electromagnetic interference as a Post-Doctoral Fellow at Carleton University, Ottawa, ON. She is currently working as a Senior Antenna Engineer on innovative designs for base station antennas in TenXc Wireless Inc., Ottawa. Her current research interests include electromagnetic theory, photonic crystals, LTCC, and system-on-package smart reconfigurable and active antennas.

Langis Roy (M'93) joined the Department of Electronics, Carleton University, Ottawa, ON, Canada, in 1999, where he is currently a Professor and since 2003 has chaired the Department. His university career began in the Department of Electrical Engineering, University of Ottawa, Ottawa, in 1993, as an Assistant Professor. During his sabbatical leave from 2005 to 2006, he was a Visiting Professor at the Valtion Teknillinen Tutkimuskeskus Micromodule Research Center, Oulu, Finland, and an Invited Professor at the Department of Electrical and Computer Engineering, Institut National des Sciences Appliquees, Toulouse, France. He is a Licensed Professional Engineer in the Province of Ontario. He collaborates extensively with industry and serves on the board of several research fund-granting agencies and technical conferences. His current research interests include integrated active antennas, numerical techniques in electromagnetic, monolithic microwave integrated circuits, low temperature co-fired ceramics, microelectromechanical systems, and radio frequency millimeter-waves.